Published in IET Control Theory and Applications
Received on 29th January 2007
Revised on 10th March 2008
doi: 10.1049/iet-cta:20070025

ISSN 1751-8644

Frequency-shaped high-gain compensator for optical disk drive control system

H.R. Kim[1] *Y. Choi*[2] *I.H. Suh*[3] *W.K. Chung*[4]

[1]*Center for Embedded Software Technology, Kyungbook National University, 1370 Sankyuk-dong Buk-gu Daegu 702-701, South Korea*
[2]*School of Electrical Engineering and Computer Science, Hanyang University, 1271 Sa3-dong Sangrok-gu Ansan 426-791, South Korea*
[3]*College of Information and Communication, Hanyang University, 17 Hangdang-dong Sungdong-gu Seoul 133-791, South Korea*
[4]*Department of Mechanical Engineering, POSTECH, San 31 Hyoja-dong Nam-gu Pohang, 790-784, South Korea*
E-mail: hrkim@cest.re.kr

Abstract: A frequency-shaped high-gain (FSHG) compensator is proposed and implemented for optical disk drive control systems, such as CD or DVD servo systems. The FSHG compensator is obtained by modifying an error-based disturbance observer. The FSHG compensator can be easily realised as a form of a low cost analogue circuit. The disturbance rejection performance can also be easily improved by filter parameters in the FSHG compensator. Design guidelines for the filter parameters (numerator order and filter time constant) are also suggested in this paper. Finally, the effectiveness of the FSHG compensator is shown through experimental results showing disturbance rejection performance evaluated under forced disturbances.

1 Introduction

An optical disk drive (ODD) such as a CD-ROM/RW requires precise servo control to read and record a large volume of data at high speed. For a high-speed and high-volume drive, there are difficult problems such as mechanical resonance, deviation of the spindle motor, external shock and eccentricity deviation of the disk. The higher the speed of the spindle motor in the ODD servo system, the worse the disturbance rejection performance of the existing controller. Currently, most controllers being operated in ODD servo systems use a lead–lead–lag compensator, which is realised in the form of a hardwired digital signal processor (DSP). However, the hardwired-DSP is only able to adjust to pole-zero locations with a fixed controller order; as a result, there is no room to realise a specially designed controller in order to improve the disturbance rejection performance. Also, since the realisation cost of the controller must be low for an ODD system application, we aim to improve the disturbance rejection performance by minimising any changes in the existing control structure.

A disturbance observer (DOB) is a viable alternative to reject disturbances caused by mechanical resonance, deviation of the spindle motor, external shock or eccentricity deviation of the disk in ODD servo systems. After the DOB estimates the equivalent disturbances, the difference between the output of the real plant and the output of the nominal plant, the estimated equivalent disturbance quantity is added to the existing control input for the cancellation of the disturbance [1]. The DOB has been widely used in the precision motion control field, for example, hard disk drive control system, because of its simple structure and good performance [2–7]. In disk drive servo systems, since only a position error signal is available, a conventional DOB was realised by attaching an additional position sensor to the original system in [8]. On the other hand, Fujiyama *et al.* showed in [9] that it was possible to construct a DOB by using only an error signal without adding an additional sensor. Also, in [10, 11], the robustness and disturbance rejection performance of a DOB system were theoretically researched and extended to the error-based DOB, however, the implementation at a low cost still remains an issue.

In this paper, the frequency-shaped high-gain (FSHG) compensator is first derived from the conventional DOB. The characteristics of the FSHG compensator become equivalent to those of the DOB if certain conditions are satisfied. Here, the conditions are derived from the high-loop-gain characteristics of the ODD servo system itself. Also, the proposed FSHG compensator has the merit that it can be implemented as an analogue circuit form. Through experimental results on the control performance against periodic disturbances caused by an eccentric disk, the effectiveness of the FSHG compensator is shown in this paper.

This paper is organised as follows: Section 2 introduces the error-based DOB in the ODD system; Section 3 explains the design guidelines of error-based DOB; Section 4 proposes the FSHG compensator, derived from the DOB, the ODD servo systems; Section 5 shows the simulation and experimental results; and finally, Section 6 draws conclusions.

2 Error-based DOB

ODD systems have dual stage motion controllers for the macro and micro actuators; the step motor is used for coarse tracking (macro) motion and the voice-coil motor for fine tracking (micro) motion, as shown in Fig. 1. Here, our main concern is the fine tracking motion, namely, the precise track following motion of the voice-coil motor. Unlike conventional control systems, the ODD control system has no reference input signal. The quantity of deviation of only an error signal from the track centre is measured according to the rotation of the optical disk. Also, since the measured error signal shows nonlinearity because of the optical reading mechanism in the ODD tracking control system, the error should be guaranteed to remain within 1/4 pitch of one track to keep its linearity. Here, most errors are caused by the disturbances by radial vibration because of eccentricity, disk surface vibration and resonance.

To improve the tracking performance of the ODD control system, the DOB is first implemented by using the programmable DSP. The main property of the DOB is that it behaves like a nominal plant component in DOB. This characteristic of the DOB has made it possible to estimate the equivalent disturbance from the modelling error, change of parameters and external disturbance. However, in the case of the ODD system, an output signal cannot be observed as distinguishable as that from the conventional system. Since the value of deviation from the track centre by the laser spot is detected and measured in a numeric form, the DOB can be reconstructed on the basis of error(ε) instead of reference(r) and output(y) as shown in Fig. 2. In the figure, the reference r and output y are virtual signals that cannot be measured in practical ODD control systems.

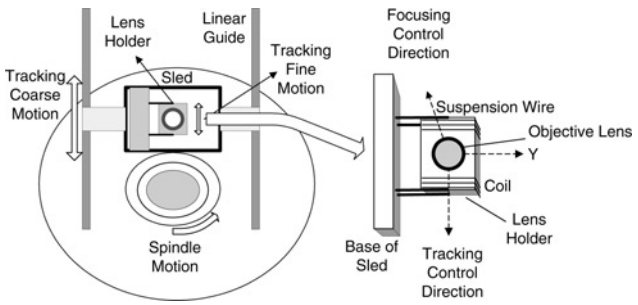

Figure 1 *Schematic diagram of ODD system*

In this figure, d_i, d_o, η and δ represent the input disturbance, output disturbance, noise and the estimated disturbance, respectively. The real plant $P(s)$ is a fifth-order system composed of the first-order driver, second-order actuator and second-order RF amplifier. The transfer function $P_n(s)$ expresses a second-order nominal plant obtained by modelling a fifth-order real plant. In addition, $Q(s)$ is a low-pass filter that is referred to as the Q filter. Now, the transfer function from the external inputs to error can be obtained as follows

$$\varepsilon = G_{d_i\varepsilon}(s)d_i + G_{d_o\varepsilon}(s)d_o + G_{\eta\varepsilon}(s)\eta \tag{1}$$

where

$$\begin{aligned} G_{d_i\varepsilon}(s) &= \frac{PP_n(1-Q)}{P_n(1-Q)+PQ+PP_nC} \\ G_{d_o\varepsilon}(s) &= \frac{P_n(1-Q)}{P_n(1-Q)+PQ+PP_nC} \\ G_{\eta\varepsilon}(s) &= \frac{PP_nC+PQ}{P_n(1-Q)+PQ+PP_nC} \end{aligned} \tag{2}$$

In the frequency region where the magnitude of the Q filter is equal to one, the transfer function in (1) will behaves approximately in the following form

$$\varepsilon = (0)d_i + (0)d_o + (1)\eta \tag{3}$$

In contrast, in the frequency region where the magnitude of the Q filter is equal to zero, the transfer function in (1) will behave approximately as follows

$$\varepsilon = \left(\frac{P}{1+PC}\right)d_i + \left(\frac{1}{1+PC}\right)d_o + \left(\frac{PC}{1+PC}\right)\eta \tag{4}$$

Equation (3) shows the main characteristic of a DOB that rejects the disturbance within the bandwidth of the Q filter. Equation (4) indicates that the DOB effects disappear out of the bandwidth of the Q filter. The effectiveness of the DOB

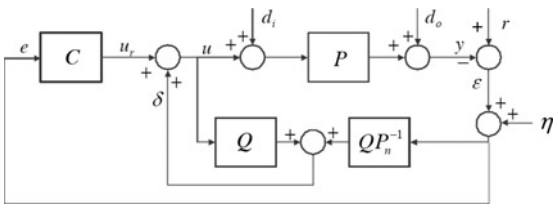

Figure 2 *Configuration of error-based DOB*

IET Control Theory Appl., 2008, Vol. 2, No. 10, pp. 851–859
doi: 10.1049/iet-cta:20070025

system was shown in [10], in which the robustness and disturbance rejection performance of the DOB according to the (numerator and denominator) orders of Q filters was proven for second-order systems. Here, the parameters of the Q filter, such as the time constant, order of the numerator/denominator and relative degree, are designed according to [10]. In this paper, the Q filter has the binomial form as follows

$$Q_{mn}(s) = \frac{\sum_{i=0}^{n} a_{mi}(\tau s)^i}{(\tau s + 1)^m} \quad \text{where} \quad a_{mi} = \frac{m!}{(m-i)!} \tag{5}$$

where τ is the time constant, m and n represent the denominator order and the numerator order satisfying $m \geq n$, respectively.

As explained, the real plant consists of a driver, actuator (voice-coil motor) and RF amplifier. However, since the bandwidths of the driver and RF amplifier are much larger than the bandwidth of the actuator, their dynamics disappear quickly and their response characteristics will not be taken into account. Here, we can obtain the second-order nominal plant in the following form

$$P_n(s) = \frac{K\omega_n^2}{s^2 + 2\zeta\omega_n s + \omega_n^2} \tag{6}$$

where K is the DC-gain of the nominal plant, ω_n the natural radian frequency and ζ the damping ratio. This nominal plant will be used to design the DOB in the following section.

3 Design guidelines of an error-based DOB

Many experiments [6, 7, 11] have reported a good disturbance rejection performance of the DOB. Now, let us assume that the nominal plant is equal to the real plant in Fig. 2. Then, we can obtain the following transfer functions

$$\begin{aligned} \varepsilon = {} & [1 - Q(s)](r - d_o) - P_n(s)u_r \\ & - [1 - Q(s)]P_n(s)d_i - Q(s)\eta \end{aligned} \tag{7}$$

Here, let us consider the transfer function from the input disturbance (d_i) to error (ε) in the equation above

$$G_{d_i\varepsilon}(s) = [1 - Q(s)]P_n(s) \tag{8}$$

then, its magnitude can be calculated by using a nominal plant (6) and Q_{mn} filter (5) as the following form

$$|G_{d_i\varepsilon}(j\omega)_{mn}| = \sqrt{\frac{k^2 c_{mn}}{((1/\omega_n^2) + (\tau\omega/\omega_n)^2)^m A\omega_n^4}}$$

where ω is the radian frequency variable

$$k \triangleq K\omega_n^2$$

$$A \triangleq \left(\frac{\omega}{\omega_n}\right)^4 + 2(2\zeta^2 - 1)\left(\frac{\omega}{\omega_n}\right)^2 + 1$$

and the coefficients c_{mn} according to Q_{mn} filters is listed in Table 1.

Now, the decibel magnitude can be obtained as follows

$$\begin{aligned} 20\log|G_{d_i\varepsilon}(j\omega)_{mn}| = {} & 20\log\left|\frac{k}{\omega_n^2}\right| \\ & - 20\log\sqrt{\left(1 - \left(\frac{\omega}{\omega_n}\right)^2\right)^2 + \left(2\zeta\frac{\omega}{\omega_n}\right)^2} \\ & + 10\log\left\{\begin{array}{c} \frac{e_{m(n+1)}}{\omega_n^{2(m-n-1)}} + \frac{e_{m(n+2)}}{\omega_n^{2(m-n-2)}}\left(\frac{\tau\omega}{\omega_n}\right)^2 \\ + \cdots + \left(\frac{\tau\omega}{\omega_n}\right)^{2(m-n-1)} \end{array}\right\} \\ & + 20(n+1)\log\left|\frac{\tau\omega}{\omega_n}\right| - 20m\log\sqrt{\frac{1}{\omega_n^2} + \left(\frac{\tau\omega}{\omega_n}\right)^2} \end{aligned} \tag{9}$$

Table 1 Coefficients c_{mn} according to Q_{mn} filters

	c_{mn}
Q_{20}	$\frac{4}{\omega_n^2}\left(\frac{\tau\omega}{\omega_n}\right)^2 + \left(\frac{\tau\omega}{\omega_n}\right)^4$
Q_{30}	$\frac{9}{\omega_n^4}\left(\frac{\tau\omega}{\omega_n}\right)^2 + \frac{3}{\omega_n^2}\left(\frac{\tau\omega}{\omega_n}\right)^4 + \left(\frac{\tau\omega}{\omega_n}\right)^6$
Q_{31}	$\frac{9}{\omega_n^2}\left(\frac{\tau\omega}{\omega_n}\right)^4 + \left(\frac{\tau\omega}{\omega_n}\right)^6$
Q_{41}	$\frac{36}{\omega_n^4}\left(\frac{\tau\omega}{\omega_n}\right)^4 + \frac{4}{\omega_n^2}\left(\frac{\tau\omega}{\omega_n}\right)^6 + \left(\frac{\tau\omega}{\omega_n}\right)^8$
Q_{42}	$\frac{16}{\omega_n^2}\left(\frac{\tau\omega}{\omega_n}\right)^6 + \left(\frac{\tau\omega}{\omega_n}\right)^8$
Q_{52}	$\frac{100}{\omega_n^4}\left(\frac{\tau\omega}{\omega_n}\right)^6 + 5\omega_n^2\left(\frac{\tau\omega}{\omega_n}\right)^8 + \left(\frac{\tau\omega}{\omega_n}\right)^{10}$
Q_{mn}	$\sum_{i=n+1}^{m} \frac{e_{mi}}{\omega_n^{2(m-i)}}\left(\frac{\tau\omega}{\omega_n}\right)^{2i}$ if $i = n+1$, $e_{mi} = a_{mi}^2$ else, $e_{mi} = a_{mi}$

To obtain insight for the design of the DOB according to Q_{mn} filters, first, let us approximate (9) in low frequencies such as $\omega \ll \omega_n$; then, (9) can be approximately given in the following form:

$$\begin{aligned} 20\log|G_{d_i\varepsilon}(j\omega)_{mn}| &\simeq 20\log\left|\frac{k}{\omega_n^2}\right| + 20\log\frac{\sqrt{e_{m(n+1)}}}{\omega_n^{m-n-1}} \\ &\quad + 20(n+1)\log\left|\frac{\tau\omega}{\omega_n}\right| - 20m\log\left|\frac{1}{\omega_n}\right| \\ &= 20\log\left|\frac{ka_{m(n+1)}}{\omega_n^2}\right| + 20(n+1)\log|\tau\omega| \end{aligned} \tag{10}$$

by using $e_{m(n+1)} = a_{m(n+1)}^2$ in Table 1. As we can see in (10), the disturbance rejection performance is dependent only on $a_{m(n+1)}$, n and τ in low frequencies. Secondly, if we approximate (9) in high frequencies such as $\omega \gg 1/\tau$, then $|G_{d_i\varepsilon}(j\omega)_{mn}|$ recovers the magnitude of nominal plant $|P_n(j\omega)|$, regardless of the Q_{mn} filters. Therefore the plot for (9) can be obtained as shown in Fig. 3. In Fig. 3, the disturbance rejection performance according to the Q_{mn} filters is depicted. Also, since most disturbances exist at low frequencies, two design guidelines can be obtained from Fig. 3 and (10).

(Guideline 1) Numerator order (n) of filter and disturbance rejection: As shown in Fig. 3, the larger the numerator order, the better the disturbance rejection performance, for example, the performance of the Q_{31} filter is better than that of the Q_{30} filter. Additionally, for Q_{mn} filters with the same numerator order, the disturbance rejection performance varies a little according to the values of $a_{m(n+1)}$ as shown in (10), for example, the Q_{20} filter shows somewhat better performance for disturbance rejection than the Q_{30} filter, because $a_{21} = 2$ for Q_{20} and $a_{31} = 3$ for Q_{30}.

(Guideline 2) Filter time constant (τ) and disturbance rejection: The filter time constant determines the effective frequency range for disturbance rejection. For instance, smaller τ means a wider frequency range for disturbance rejection. As shown in Fig. 3, since the second-order plant (6) has the advantage of -40 db/decade roll-off in high frequencies over the natural radian frequency ω_n, we should determine the time constant, τ, with $\tau < 1/\omega_n$.

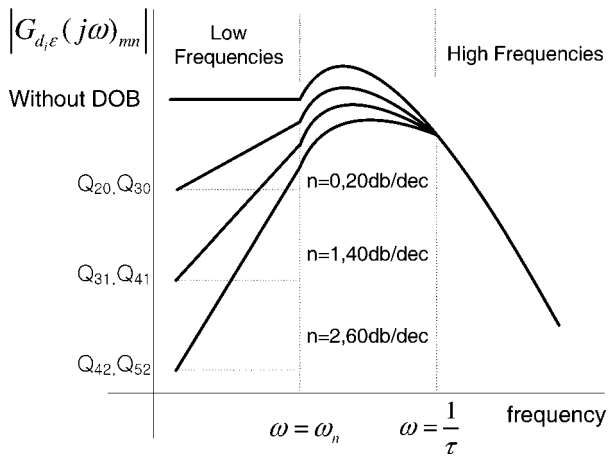

Figure 3 *Disturbance rejection performance according to the numerator order of Q_{mn} filters*

The two guidelines can be used for the design parameters (numerator order and filter time constant) of Q filter in the error-based DOB. For example, if the disturbance rejection performance is important in designing the DOB, the numerator order should be increased according to (Guideline 1). Also, if the disturbance rejection range is important in designing the DOB, the filter time constant should be adjusted according to (Guideline 2). In the following section, we propose an FSHG compensator obtained by using the characteristics of the ODD servo system.

4 FSHG compensator

Although the DOB shows good performance for disturbance rejection, industry has not used DOB because its implementation requires additional DSP at a high cost. The conventional (lead–lead–lag) controller has the following form

$$C(s) = K_c\frac{(1+s/z_1)(1+s/z_2)(1+s/z_3)}{(1+s/p_1)(1+s/p_2)(1+s/p_3)} \tag{11}$$

where K_c is the proportional gain, $-p_i$ the adjustable pole location and $-z_i$ the adjustable zero location for $i = 1, 2, 3$. The discrete form of a conventional (lead–lead–lag) controller (11) is realised by hardwired-DSP as depicted in Fig. 4. The control parameters from k_{tn1} to k_{tn18} in Fig. 4 determine the poles and zeros of a discrete lead–lead–lag controller. Since the existing controller in the ODD servo system has a fixed form, the DOB cannot be implemented in the existing controller. In this respect, we need to devise the implementation method at a low cost, and we begin by looking into the characteristics of the ODD system itself. In the ODD system, if the magnitude of the error signal is within ± 1 V error, the output of the QP_n^{-1} block in the DOB maintains the level of approximately ± 0.1 mV because the real and nominal plants have a DC-gain of approximately 80 dB ($= 10^4$). Here, a 1 V error corresponds to a tracking error of 0.424 μm because the RF amplifier has a sensitivity of 2.34 V/μm to read the tracking error. However, this can be a trivial value because the analogue-to-digital converter cannot detect a small change. Although it is known that the

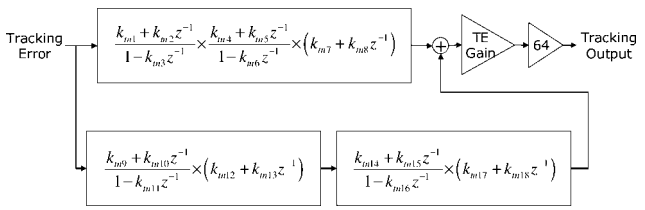

Figure 4 *Block diagram of hardwired DSP controller*

IET Control Theory Appl., 2008, Vol. 2, No. 10, pp. 851–859
doi: 10.1049/iet-cta:20070025

QP_n^{-1} block plays an important role in the DOB system, the QP_n^{-1} block does not significantly affect the ODD system. From this point of view, the DOB can be modified as shown in Fig. 5, and we call it an FSHG compensator.

The FSHG compensator has been derived from the DOB and the characteristics of the ODD system itself. The transfer functions obtained by using the FSHG compensator are as follows

$$G_{d_i\varepsilon}(s) = \frac{P(1-Q)}{1-Q+PC}$$
$$G_{d_o\varepsilon}(s) = \frac{(1-Q)}{1-Q+PC} \quad (12)$$
$$G_{\eta\varepsilon}(s) = \frac{PC}{1-Q+PC}$$

As shown in (12), if $Q = 1$ in the low frequencies, then the FSHG compensator shows the disturbance rejection property. In other words, the FSHG compensator does not lose the characteristics of a DOB in view of the disturbance rejection performance and sensor noise effect. However, the one characteristic that makes the real plant behave like a nominal plant in the DOB disappears in the FSHG compensator system. Actually, the FSHG compensator has the structure of a high-gain controller with frequency shaping. If a plant has high DC-gain, the DOB has this characteristic because the QP_n^{-1} block can be neglected in the DOB itself.

The transfer functions of the DOB and the FSHG compensator are summarised by using (2) and (12) in Table 2, in which the equations in (2) are divided by P_n.

In Table 2, the transfer functions of the DOB can be approximated to the transfer functions of the FSHG if the following conditions are satisfied

$$\text{(condition 1)} \quad |1-Q+PC| \gg |PP_n^{-1}Q| \quad (13)$$
$$\text{(condition 2)} \quad |PC| \gg |PP_n^{-1}Q| \quad (14)$$

where $|\cdot|$ is the magnitude of the corresponding transfer function.

To make the analysis easier, if we assume that the transfer function of the nominal plant is equal to that of a real plant,

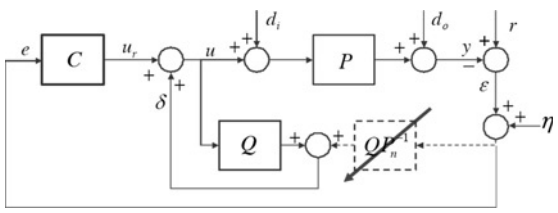

Figure 5 *Structure of FSHG compensator*

Table 2 Transfer functions of DOB and FSHG

	DOB	FSHG
$G_{r\varepsilon}$	$\frac{PC+PP_n^{-1}Q}{1-Q+PC+PP_n^{-1}Q}$	$\frac{PC}{1-Q+PC}$
$G_{d_i\varepsilon}$	$\frac{P(1-Q)}{1-Q+PC+PP_n^{-1}Q}$	$\frac{P(1-Q)}{1-Q+PC}$
$G_{d_o\varepsilon}$	$\frac{(1-Q)}{1-Q+PC+PP_n^{-1}Q}$	$\frac{(1-Q)}{1-Q+PC}$
$G_{\eta\varepsilon}$	$\frac{PC+PP_n^{-1}Q}{1-Q+PC+PP_n^{-1}Q}$	$\frac{PC}{1-Q+PC}$

then (13) can be simplified to the following form

$$|1-Q+PC| \gg |Q| \quad (15)$$

Since $(1+PC)$ indicates the inverse of the sensitivity function of the original system, the above equation can be changed as follows

$$\left|\frac{1}{S_n} - Q\right| \gg |Q| \quad (16)$$

Also, since the Q filter has the form of a low-pass filter, the following inequality can be obtained for low frequencies satisfying $|Q| = 1$

$$\text{(revised condition 1)} \quad |1/S_n - Q| \gg 1 \quad \text{for low frequencies} \quad (17)$$

The revised condition 1 is valid under the cut-off frequency of the Q filter. The suggested one can be applied to the cut-off frequency of the Q filter. Therefore the Q filter should be chosen to satisfy the condition of (17), that is, the magnitude of $|1/S_n - Q|$ should be >1. This is the physical meaning obtained from revised condition 1. On the other hand, dividing both sides of (14) by the $|P|$ gives the following relation

$$\text{(revised condition 2)} \quad |C| \gg |P_n^{-1}Q| \quad (18)$$

Equation (18) describes the condition where the magnitude of the given controller is greater than the magnitude of QP_n^{-1}. If the DC-gain of the nominal plant is very large, the magnitude of QP_n^{-1} is relatively small; this becomes identical to the previous explanations. As a result, if two conditions of (17) and (18) are satisfied for the given systems, the DOB can be substituted with the FSHG compensator while retaining properties of the original DOB.

5 Experimental results

The DVD-ROM drive is used as an example for the simulations and experiments using the DOB and the

FSHG. The nominal plant of an ODD system has the form of (6), where ω_n is 314.16 rad/s, ζ is 0.3155 and K is 7.79×10^3. The conventional lead–lead–lag controller embedded in the ODD system itself has the following form

$$C(s) = \frac{9.44 \times 10^{-12}s^3 + 2.88 \times 10^{-7}s^2 + 0.00025s + 5}{5.99 \times 10^{-13}s^3 + 7.09 \times 10^{-7}s^2 + 0.00021s + 1} \tag{19}$$

The Q filter has the form of (5) for the DOB and the FSHG, and the time constant of the filter is set to 1.989×10^{-4} s. To compare the real plant with the nominal plant, Bode plots are drawn as shown in Fig. 6*a*. The nominal model coincides with the real plant except for a high-frequency region. First, the conditions of application of the FSHG compensator such as (13), (17) and (18) must be checked. Figs. 6*b*–*d* show that the conditions of application of the FSHG are satisfied for the given system. In Fig. 6*c*, the condition of (17) is satisfied within the low frequencies. Also, since the DC-gain of the ODD system is up to 80 dB, the magnitude of the controller is greater than that of QP_n^{-1} as shown in Fig. 6*d*. Therefore the FSHG compensator can be applied to the suggested ODD system instead of the DOB. In Fig. 7, the sensitivity functions of the DOB and FSHG are compared; in fact, the Bode plots of the two systems are almost in accord. Also, the disturbance rejection performance changes according to the numerator/denominator orders of the Q filter. As suggested in (Guideline 1), as the numerator order of the Q filter increases, the disturbance rejection performance improves as shown in Fig. 7. In addition, the frequency responses can be obtained for the conventional ODD control system, conventional ODD control system with the

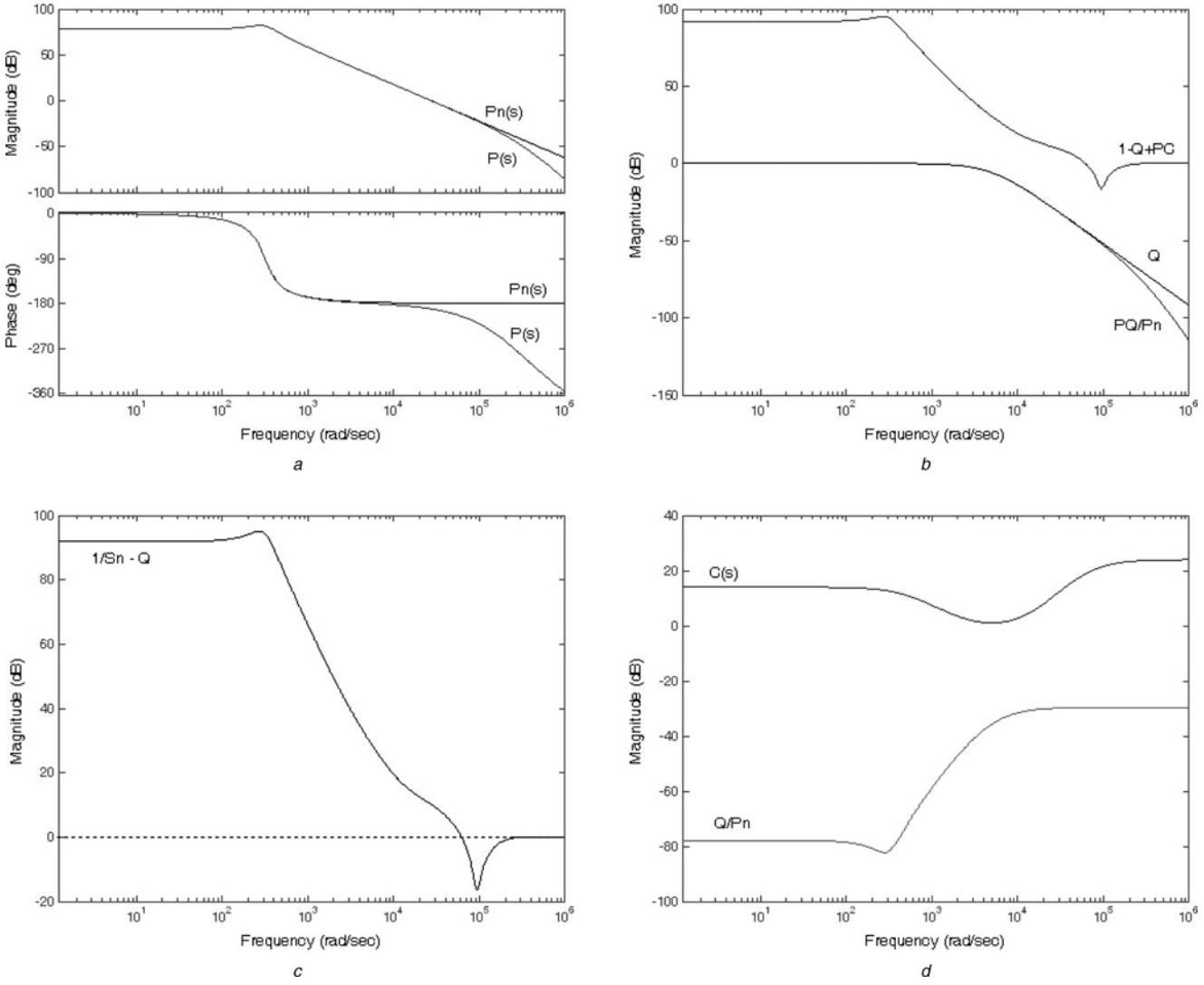

Figure 6 *Bode plots of several transfer functions*

a $P(s)$ against $P_n(s)$
b $(1 - Q + PC)$ against $PP_n^{-1}Q$
c $|1/S_n - Q|$
d $|C(s)|$ against $|QP_n^{-1}|$

IET Control Theory Appl., 2008, Vol. 2, No. 10, pp. 851–859
doi: 10.1049/iet-cta:20070025

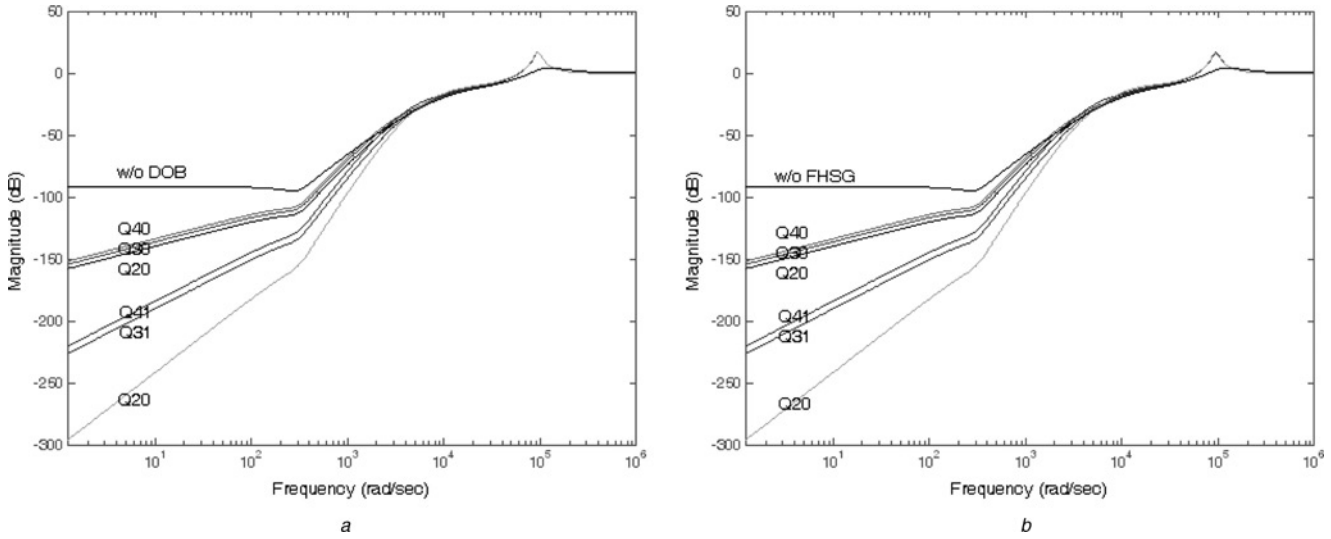

Figure 7 *Sensitivity functions of DOB and FSHG compensator*
a DOB
b FSHG

DOB and conventional ODD control system with the FSHG compensator as shown in Fig. 8, respectively. From these frequency responses, we are able to obtain the gain/phase margins as follows:

- Conventional control system: GM infinity; PM 45.68°

- Conventional control system + DOB or FSHG: GM infinity; PM 45.73°

Here, we can confirm that the adding of the DOB and FSHG do not affect the gain and phase margins. Therefore we could design the FSHG compensator such that it could keep the ODD control system stably and tolerably from external disturbances caused by disk eccentricity and an external impact without degrading the specifications (gain margin and phase margin) of the existing lead–lead–lag controller.

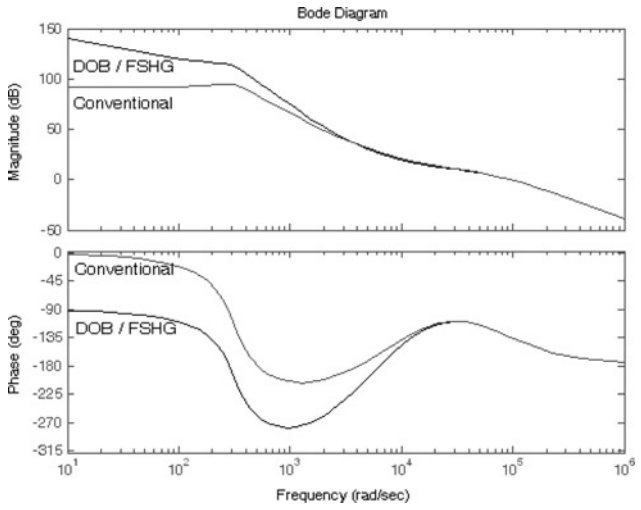

Figure 8 *Comparison of magnitude and phase changes using DOB or FSHG*

The experimental results are explained as follows. First, the DOB was realised by using the programmable-DSP M44. The control frequency of the lead–lead–lag compensator embedded in the ODD systems was very high (it was 176.4 kHz). However, the control frequency of the DOB was set to 20 kHz because of the hardware limitation of M44 DSP. Secondly, the FSHG compensator was implemented by using cheap analogue operational amplifiers (OP-AMP) as shown in Fig. 9. The analogue FSHG compensator was simply composed of the second-order Q filter and an add-on circuit. Four OP-AMPs were used to construct the Q filter and adder circuit. In addition, the analogue switch was utilised to distinguish between the search mode and tracking mode in the ODD system. The search mode appears when the actuator moves across the tracks and the generated error signal is nonlinear. On the other hand, the tracking mode appears when the actuator follows the track and the generated error signal is linear. In the tracking mode, the switch becomes ON and the FSHG compensator starts.

To inject the forced disturbance into the ODD servo system, the commercial 150 μm DVD eccentricity disk was used. In the experiment, the Q_{31} filter was adopted since it had excellent disturbance rejection performance through simulation. Furthermore, the cut-off frequency of the Q filter is set to 800 Hz because the ODD system rotates up to a maximum speed of 160 Hz. As shown in Fig. 10*a*, the commercial ODD system was affected by the disturbances caused by the eccentric disk. Its magnitude was up to 640 mV. The experimental results of the DOB and the FSHG compensator show the performance improvement as shown in Figs. 10*b* and 10*c*.

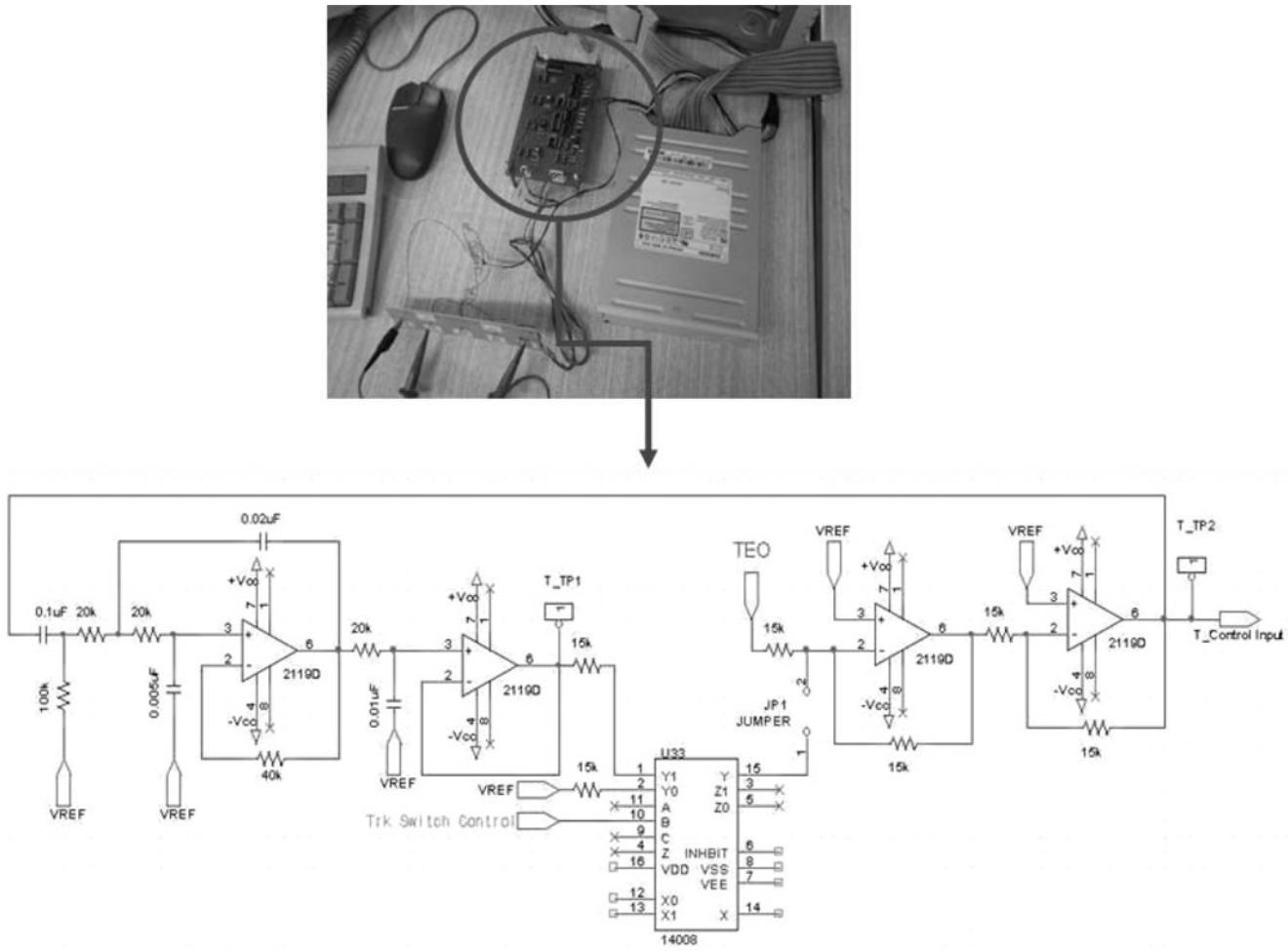

Figure 9 *Experimental apparatus of an analogue FSHG compensator*

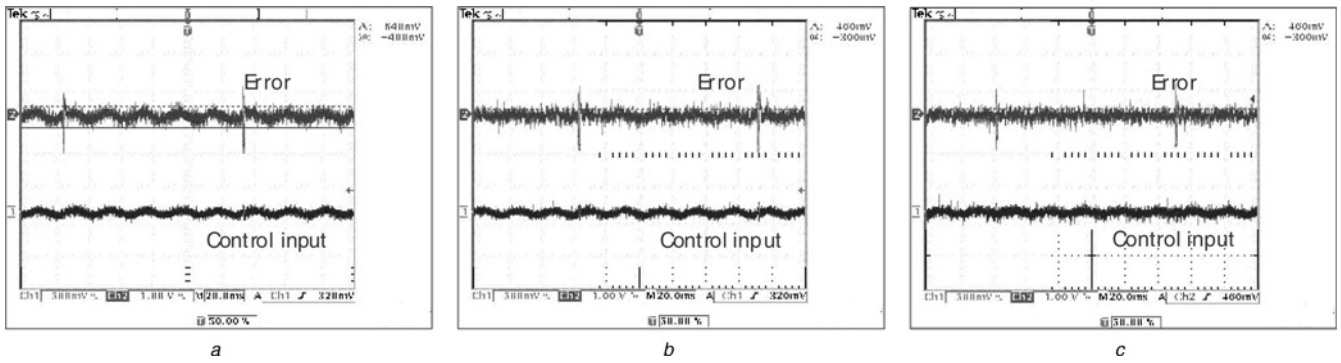

a *b* *c*

Figure 10 *Experimental results for disturbance rejection performance*

a Conventional ODD system
b When DOB is attached
c When FSHG is attached

The magnitudes of the DOB and the FSHG decreased to 500 mV. In the case of a conventional ODD control system, the error signal has a periodic form according to the rotation of the spindle motor with the eccentric disk. However, in the case of the DOB and the FSHG, the periodic error signals disappear because of the disturbance rejection performance of the FSHG compensator. Therefore we can conclude that the DOB and the FSHG show the same performance for disturbance rejection of the ODD system. Moreover, the FSHG compensator has the additional advantage of being implemented simply by using cheap analogue elements.

IET Control Theory Appl., 2008, Vol. 2, No. 10, pp. 851–859

doi: 10.1049/iet-cta:20070025

6 Conclusion

In this paper, an FSHG compensator was proposed using the concept of an error-based DOB and realised as a form of an add-on analogue circuit at a low cost. Also, the disturbance rejection performance was easily improved by adjusting the filter parameters (numerator order and filter time constant) in the FSHG compensator. Finally, the effectiveness of the FSHG compensator was proved through the experimental results showing disturbance rejection performance evaluated under forced disturbances.

7 Acknowledgment

This work was supported in part by the Gyunggi Regional Research Center Program under Grant 2007-000-0407-0003. All correspondences should be addressed to Il Hong Suh.

8 References

[1] OHNISHI K.: 'A new servo method in mechatronics', *Trans. Jpn. Soc. Electr. Eng.*, 1987, **107-D**, pp. 83–86

[2] LEE H.S., TOMIZUKA M.: 'Robust motion controller design for high-accuracy positioning systems', *IEEE Trans. Ind. Electron.*, 1996, **43**, (1), pp. 48–55

[3] OHNISHI K., SHIBATA M., MURAKAMI T.: 'Motion control for advanced mechatronics', *IEEE/ASME Trans. Mechatronics*, 1996, **1**, (1), pp. 56–67

[4] IWASAKI M., SHIBATA T., MATSUI N.: 'Disturbance-observer-based nonlinear friction compensation in table drive system', *IEEE/ASME Trans. Mechatronics*, 1999, **4**, (1), pp. 3–8

[5] KEMPF C.J., KOBAYASHI S.: 'Disturbance observer and feedforward design for a high-speed direct-drive positioning table', *IEEE Trans. Control Syst. Technol.*, 1999, **7**, (5), pp. 513–526

[6] TESFAYE A., LEE H.S., TOMIZUKA M.: 'Sensitivity optimization approach to design of a disturbance observer in digital motion control system', *IEEE/ASME Trans. Mechatronics*, 2000, **5**, (1), pp. 32–38

[7] WHITE M., TOMIZUKA M., SMITH C.: 'Improved track following in magnetic disk drives using disturbance observer', *IEEE/ASME Trans. Mechatronics*, 2000, **5**, (1), pp. 3–11

[8] UEDA J., IMAGI A., TAMAYAMA T.: 'Tracking following control of large capacity flexible disk drive with disturbance observer using two position sensors'. Proc. Int Conf. Advanced Intelligent Mechatronics, 1999, pp. 144–149

[9] FUJIYAMA K., TOMIZUKA M., KATAYAMA R.: 'Digital tracking controller design For CD player using disturbance observer'. Proc. Int. Workshop on Advanced Motion Control, 2000, pp. 141–146

[10] CHOI Y., YANG K., CHUNG W.K., KIM H.R., SUH I.H.: 'On the robustness and performance of disturbance observer for second-order systems', *IEEE Trans. Autom. Control*, 2003, **48**, (2), pp. 315–320

[11] YANG K., CHOI Y., CHUNG W.K.: 'On the tracking performance improvement of optical disk drive servo systems using error-based disturbance observer', *IEEE Trans. Ind. Electron.*, 2005, **52**, (1), pp. 270–279